Available online at www.sciencedirect.com
SCIENCE DIRECT
Journal of Photochemistry and Photobiology A: Chemistry 178 (2006) 185–191
Journal of Photochemistry and Photobiology A:Chemistry
www.elsevier.com/locate/jphotochem

Photoinduced interlayer electron transfer in alternating porphyrin–fullerene dyad and regioregular poly(3-hexylthiophene) Langmuir–Blodgett films

Tommi Vuorinen *, Kimmo Kaunisto, Nikolai V. Tkachenko, Alexander Efimov, Helge Lemmetyinen

Institute of Materials Chemistry, Tampere University of Technology, P.O. Box 541, 33101 Tampere, Finland

Available online 22 November 2005

Abstract

Alternating Langmuir–Blodgett (LB) bi-layer structures containing a donor–acceptor (DA) dyad layer and a layer of conducting polymer were used to study interlayer vectorial photoinduced electron transfer (VPET). The used porphyrin–fullerene dyads were known to be capable of VPET, from the porphyrin to fullerene moiety, as a LB monolayer structure. The DA dyad and the poly(3-hexylthiophene), PHT, layers were deposited as adjacent LB monolayers in order to promote the secondary electron transfer from the polymer to the porphyrin cation, the product of the primary electron transfer. The VPET reaction was studied with the time-resolved Maxwell displacement charge (TRMDC) method both in the photovoltage (PV) and photocurrent (PC) modes. The PHT monolayer at the side of the porphyrin moieties lengthened the charge separation (CS) distance. Because of PHT the photovoltage amplitudes were increased and the recombination kinetics of the charge-separated state was delayed. The electron transfer direction in the bi-layer system was determined by the orientation of the DA dyad. The charge separation in the system took place with yield close to unity.

Keywords: Electron transfer; LB film; Porphyrin; Fullerene; Polythiophene

1. Introduction

Design and study of molecular systems capable for intramolecular photoinduced electron transfer have importance when new types of organic photovoltaic (PV) materials are searched [1–3]. Efficient photoinduced charge separation (CS) is an essential event for the light-to-electricity conversion. The efficient intramolecular CS can be achieved by using donor–acceptor (DA) molecules in which the electron donor and acceptor moieties have been linked covalently together [4–7]. In addition to dyads, more advanced molecular systems, such as triads and tetrads, have been synthesized and their electron transfer properties studied [8–13]. In fabrication of DA dyads two very widely used compounds are fullerene and porphyrin [1,14–19]. The studies have shown that the intramolecular charge transfer in this kind of DA molecules takes place with high yield in dilute solutions [14,20]. To utilize the intramolecular charge separation in light conversion one has to immobilize the DA molecules as ordered molecular films. A widely used method to assemble molecular monolayers and deposit them to form a solid multilayer structure is the Langmuir–Blodgett (LB) technique [21]. Although the technique sets specific requirements for the molecules and thereby limits its applicability, the LB technique is a powerful and inexpensive method to engineer different molecular interfaces. The defined orientation of the DA molecules in an LB monolayer enables a vectorial charge transfer in the system [22–24]. Yamazaki and co-workers have studied the electric field effect on the photoinduced vectorial interlayer energy and electron transfer processes in LB films by fluorescence method [25,26].

A molecular photovoltaic device can be imagined to consist of series of interacting layers with different functions [24]. The principal part of the device is the donor–acceptor interface where the primary photoinduced charge separation takes place. The charges generated in the DA interface should be quickly evacuated from each other and delivered to the electric circuit to avoid losses due to the charge recombination. A simplest device working as presented consists of three functional layers placed in between electrodes: a hole transport layer, a donor–acceptor layer and an electron transport layer. For this structure one can count several reactions and processes which take place in the device after the photoexcitation. Those are the

* Corresponding author. Tel.: +358 3 3115 3629; fax: +358 3 3115 2108.
E-mail address: tommi.vuorinen@tut.fi (T. Vuorinen).

1010-6030/$ – see front matter © 2005 Elsevier B.V. All rights reserved.
doi:10.1016/j.jphotochem.2005.10.014

primary charge separation in the donor–acceptor layer, electron capture and electron transport by the electron transport layer, and the electron transfer to the anode, and analogously, the hole capture, transport and transfer to the cathode by the hole transfer layer. A coherent performance of all these functions is essential for the operation of the device. Due to the complex function of the device it is important to study and analyze carefully all the processes involved. In the present work, the model samples were prepared in order to study the processes mentioned above, and specially the primary CS in the DA layer and the hole capture by the hole transport layer.

Previously we introduced donor–acceptor dyads composed of porphyrin and fullerene moieties covalently linked together with two molecule chains [15]. The dyads have polar groups either in the porphyrin or in the fullerene end of the molecule to enable the LB film fabrication. When the dyads were incorporated into the LB films, the photoinduced vectorial electron transfer was observed in direction from porphyrin to fullerene [27]. For the monolayers consisting of dyads having the hydrophilic groups in the porphyrin end of the molecule the recombination of charges obeyed a power law, $N_{CS}(t) \sim t^{-b}$, with $b \approx 0.25$. In addition, the photoinduced charge separation was considerably longer living in films than in solution [20,27]. In this work the monolayer of the dyad with the hydrophilic groups in the porphyrin end was deposited on a secondary electron donating, or hole transport layer, conducting polymer. The polymer was polyhexylthiophene (PHT) which is known to have a p-type semiconductor character [28]. The main focus of the present paper is on the characterization of the electron donation and the hole capture process by means of the time-resolved Maxwell displacement charge (TRMDC) method.

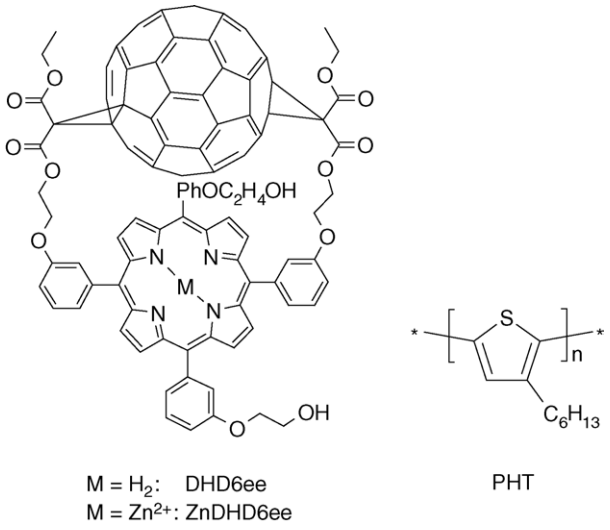

Scheme 1.

2. Materials and methods

2.1. Materials

Chloroform of analytical grade (Merck) was used for solution preparation and spreading solvent without any further purification. Matrix molecule for the LB film, octadecylamine (ODA), was of 99% grade (Sigma). The synthesis for the studied dyad molecules is described elsewhere [15]. The structures for the dyads, DHD6ee and its zinc derivative, and the regioregular poly(3-hexylthiophene), PHT, are presented in Scheme 1. PHT was purchased from Aldrich and was of 98.5% grade. The chloroform solutions were prepared to have concentrations of approximately 1 mg ml^{-1} of dyad or ODA and 0.2 mg ml^{-1} of PHT. The spreading solutions were diluted from these stock solutions to the total concentration $\leq$1.0 mM.

2.2. Sample preparation

The LB 5000 and LB Minitrough systems (KSV Instruments, Helsinki, Finland) were used for the isotherm measurements and the film depositions. The subphase was a phosphate buffer containing 0.5 mM Na_2HPO_4 and 0.1 mM NaH_2PO_4 (pH $\sim$ 7) in ion-exchanged Milli-Q water. The subphase temperature was adjusted with a thermostat to 18 ± 0.5 °C. Samples for spectroscopic studies were deposited onto quartz substrates which were cleaned by the standard procedure [21] and plasma etched for 15 min in a low-pressure nitrogen atmosphere with plasma cleaner PDC-23G (Harrick). For the photoelectrical measurements glass slides covered by semitransparent ITO electrode with sheet resistance approximately 10 Ω per square were used. The glasses with ITO electrodes were cleaned in ultrasonic bath first in acetone and then in chloroform and plasma etched in nitrogen for 10 min prior to use.

The film formation and the deposition conditions for the dyads are described in details elsewhere [27]. In this work the dyad concentrations in LB film preparation were 10 and 18 mol% in ODA for DHD6ee and ZnDHD6ee, respectively. The dyad monolayer deposition was done at the surface pressure of 15 mN m^{-1} with deposition rates of 5 mm min^{-1} in both directions. For the LB deposition of PHT it was mixed with ODA at concentration of 60 mol%, counted per PHT monomer unit. The PHT deposition pressure was 20 mN m^{-1} and the deposition rates were 7 and 4 mm min^{-1} for the water-to-air (up) and air-to-water (down) depositions, respectively [23].

A general structure of the sample for electrical measurements was ITO|insulating ODA layers|active layers|insulating ODA layers|top electrode, where the top electrode was either a drop of indium–gallium liquid allow (InGa) or a solid evaporated aluminum electrode. When aluminum electrodes were evaporated onto sample, the ITO electrode was removed from half of the substrate by 50% aqua regia at 50 °C prior to any other operations. Eleven layers of ODA were deposited onto the ITO slides to prevent interactions between the active layers and the ITO electrode. After the active layer deposition, 12 ODA layers were deposited onto the sample in order to prevent interactions between the active molecules and the InGa electrode. When Al electrodes were evaporated the active layers were covered with 20 protective ODA layers.

Thermal evaporation of Al top electrodes was done in high vacuum ($p < 10^{-5}$ mbar) with BOC Edwards Auto 306 coating system. The used evaporation source was a tungsten filament. The Al deposition rate was 0.1–0.3 nm s^{-1} and the thickness of

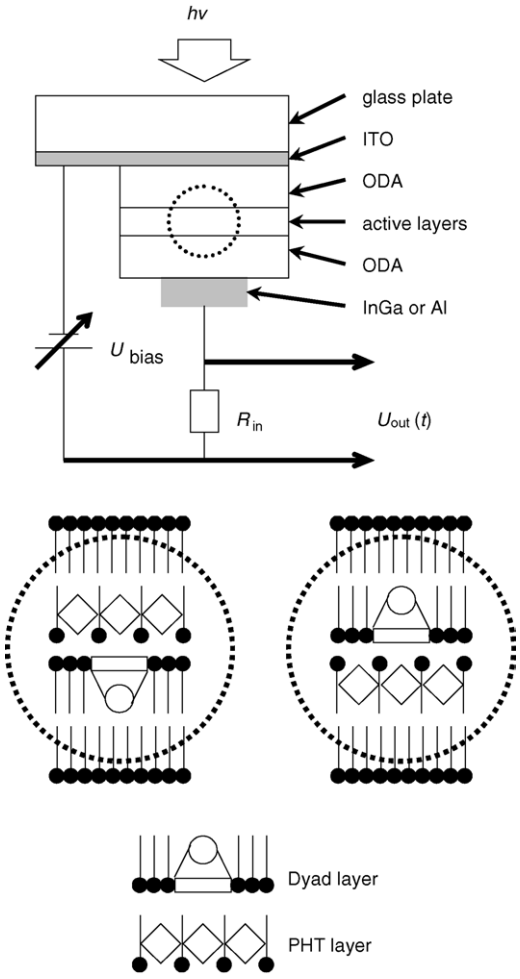

Scheme 2.

the top electrode approximately 50 nm. The preliminary tests showed that in average Al was penetrated through the five top layers during the evaporation. The Al top electrode had roughly 1 mm^2 overlapping area with the ITO bottom electrode and the exact area was determined for individual Al electrode.

2.3. Absorption measurements

The absorption spectra of the films were recorded by a Shimadzu UV-2501 PC spectrophotometer.

2.4. Electrical measurements

The vectorial photoinduced electron transfer (VPET) was studied with the time-resolved Maxwell displacement charge method [22,29]. A scheme for the measurement circuit and a sample structure are shown in Scheme 2. Since the photoactive layers are insulated from the electrodes, the measured TRMDC signals are caused only by photoinduced electron movements inside the active layers and perpendicular to the plane of the film. The sequence for the active species in the PHT–dyad bi-layers was PHT–porphyrin–fullerene. For both dyads, the bi-layer sample pairs with opposite orientations in respect of the electrodes were prepared. The samples had extremely low conductivity ($R_s > 10^{12}$ Ω) and therefore they could be treated as capacitors with a capacitance, C_s, typically 100–200 pF. The pre-amplifier input resistance (R_{in}) was 100 MΩ or 10 GΩ. All electrical measurements were done without external electric field, i.e. $U_{bias} = 0$.

The TRMDC measurements were carried out both in the photovoltage and photocurrent (PC) modes. The essential difference between the PV and PC modes is the used time domain. The time limit between these two modes is the instrumental time constant $\tau_{RC} = R_{in}C_s$. When the measurements are carried out in much shorter time than τ_{RC}, i.e. in the PV mode, the change of the voltage over the capacitor formed by the sample due to the current in the external measuring circuit is negligible. Thus, the transient voltage amplitude is proportional to the density of charge-separated states since the only path for the voltage over the capacitor to relax, during time shorter than τ_{RC}, is the charge recombination in the active layer. When the measurements are carried out in the photocurrent mode the used time domain is much longer than τ_{RC} and thus the voltage over the sample was virtually zero. In the PC mode, the current through the external circuit is measured. The transient photocurrent is proportional to the formation/relaxation rate of CS states. In time range close to τ_{RC} a more complex analysis should be used.

In the PV mode, the samples were excited by 5 ns laser pulses from second harmonic of a titanium–sapphire laser (adjustable in range of 410–450 nm) pumped by the second harmonic of a Q-switched Nd:YAG laser (532 nm). The time resolution for the PV measurements was approximately 10 ns. In the PC mode, the samples were excited step-wise by the light from an arc lamp. The excitation wavelength for the PC measurements was selected either by a set of color filters or by a monochromator. The maximum transmission for the color filter set was 430 nm and bandwidth approximately 30 nm. The maximum excitation power density at the sample was ca. 5 mW cm^{-2}. When the photocurrent action spectra were recorded a monochromator was used to select the excitation wavelength. The wavelength range for the action spectra measurements was 390–620 nm with the steps of 10 nm except in the Soret band region where the steps were 5 nm. In both PV and PC modes, the excitation power density was adjusted with a set of neutral density filters.

3. Results and discussion

3.1. UV–vis absorption

The absorption spectra of DHD6ee and PHT monolayers and PHT–DHD6ee bi-layers are presented in Fig. 1. For the DHD6ee LB monolayer a 4 nm (from 428 to 432 nm) red shift of the Soret band was observed compared to the spectrum in toluene [27]. For the PHT–DHD6ee the Soret band is less red shifted to 429 nm and the absorbance increased 10% compared to the dyad monolayer. One explanation for the smaller red shift in the bi-layer is the interaction between porphyrin and PHT. The PHT film has a broad absorption band with the maximum at 530 nm. Both the porphyrin and the PHT absorptions are well-pronounced in the bi-layer spectrum.

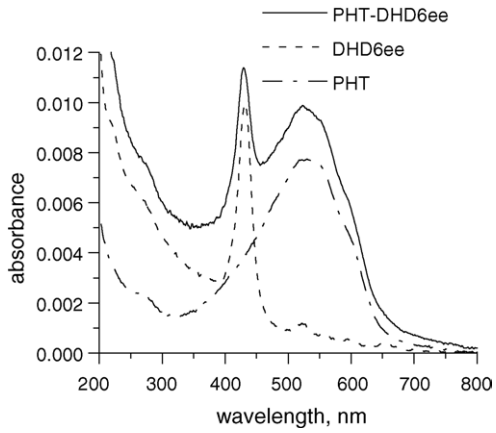

Fig. 1. Absorption spectra for the DHD6ee and PHT monolayers and for the PHT–DHD6ee bi-layer obtained by dividing the spectra of corresponding multilayer samples by the number of the layers.

3.2. Electrical measurements

The photoinduced electron transfer in the DHD6ee and ZnDHD6ee monolayers was studied earlier [27]. In this work, the PHT layers were added in the film structures adjacent to the dyad layer in order to create an interaction between the layers and a longer charge separation distance in the molecular system. Previously we have demonstrated that PHT can act as an electron donor for the phytochlorin–fullerene dyads in the alternating bi-layer structures [23,24]. In this study, the monolayer of PHT and the dyad were deposited one after another, in order to create a chromophoric triad structure with sequence PHT–porphyrin–fullerene.

3.2.1. Photovoltage response

The PHT monolayer had similar effect on the photovoltage response of DHD6ee and its zinc derivative as was observed for the phytochlorin–fullerene dyads [23]. As can be seen in Fig. 2a, addition of a PHT layer increases the maximum photovoltage amplitude 3.5-fold as well as the lifetime of the charge-separated state (Fig. 2b). The increase in the amplitude indicates a longer charge separation distance [24]. In addition, the longer distance between the separated charges slows down the charge recombination and thus longer living CS state is obtained for the triad compared to the dyad system. Thus, the primary charge separation in the dyad layer is prolonged by the secondary electron transfer from PHT to the porphyrin cation.

Fig. 3 presents the dependence of the maximum photovoltage response amplitude (U_{out}) on the excitation energy density (I_{exc}). The PV amplitude has the dependence $U_{out} = U_0(1 - \exp[-I_{exc}/I_0])$ on the excitation density with the saturation amplitude (U_0) and the saturation excitation density (I_0) [27]. At the low excitation densities the U_{out} versus I_{exc} dependence can be approximated to be linear, $U_{out} = sI_{exc}$. The initial slope, s, is proportional to the absorption at the excitation wavelength, the number of the charge-separated states (N_{CS}), and the distance of the charge separation (d) [24]. The initial slopes for the DHD6ee and ZnDHD6ee monolayers are 0.95 and 1.19 V mJ^{-1} cm^2, respectively [27]. When the dyad monolayers

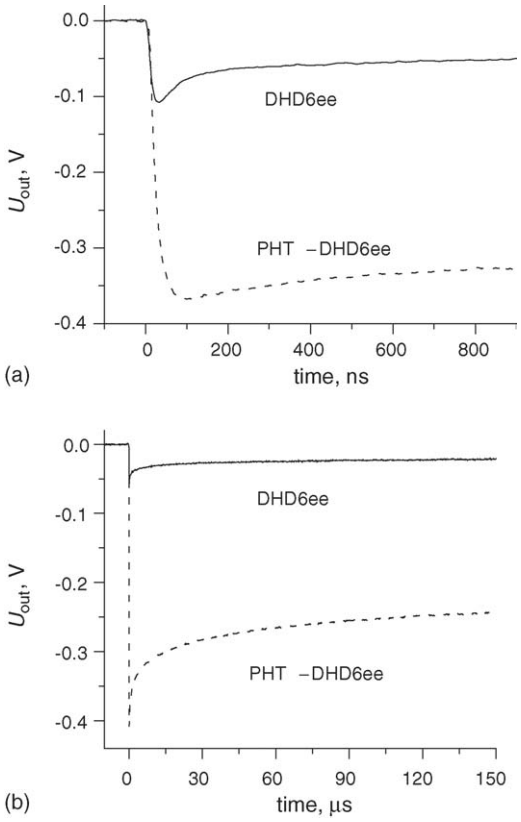

Fig. 2. (a and b) Photovoltage responses for the DHD6ee (up) and PHT (down)/DHD6ee (up) samples in two-time scales.

are combined with the PHT monolayer the slopes increase to values of 3.14 and 4.08 V mJ^{-1} cm^2 for the PHT–DHD6ee and PHT–ZnDHD6ee bi-layers, respectively, being for the bi-layer samples approximately 3.3 times as high as for the corresponding monolayers. The porphyrin absorptions at the excitation wavelength are practically the same in both structures, as seen in Fig. 1. The charge separation distance in the dyad monolayer is estimated to be 0.5 nm [27], but lengthened in the PHT–dyad bi-layer. The thickness of 60 mol% PHT monolayer is circa 3 nm [30]. Thus, one can consider that the average increase in the

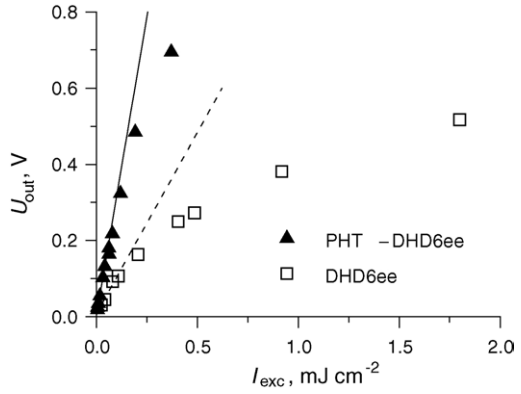

Fig. 3. Dependence of photovoltage on the excitation density for the DHD6ee monolayer and the PHT–DHD6ee bi-layer and the initial slopes obtained from the curves. The DHD6ee monolayer was deposited in both samples in the water-to-air direction.

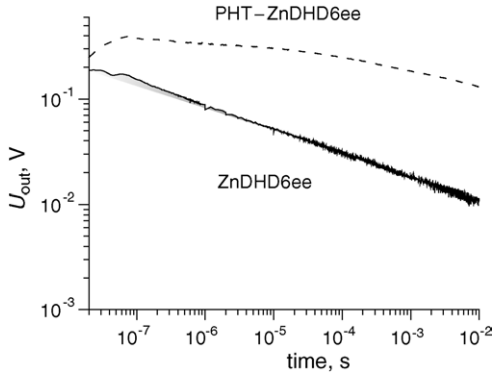

Fig. 4. Photovoltage decays for the ZnDHD6ee monolayer and PHT–ZnDHD6ee bi-layer. The dyad is deposited in the water-to-air direction. Excitation energy density for dyad was 0.15 and for bi-layer 0.25 mJ cm^{-2}. R_{in} = 10 GΩ.

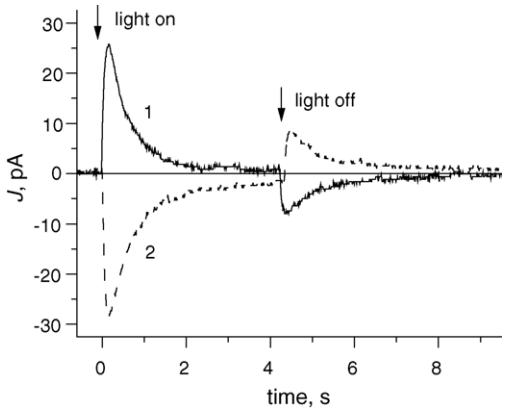

Fig. 5. Photocurrent responses for complementary PHT–DHD6ee bi-layer samples. Sample 1 (solid line) has the sequence for the active species ITO|fullerene–porphyrin–PHT and sample 2 (dashed line) ITO|PHT–porphyrin–fullerene. The excitation power density was 5 mW cm^{-2}.

electron transfer distance is half of the polymer layer thickness, i.e. 1.5 nm. For the PHT–dyad bi-layers the distance d can be estimated to be 2 nm, i.e. four times longer than that for the dyad alone. The increased charge transfer distance could result in four times as high signal for the bi-layer structure as for the dyad monolayer. According to this estimation, and taking the increase in the initial slopes of U_{out} versus I_{exc} curves into account, the yield of the secondary electron transfer from PHT to the porphyrin cation could be at least 80%.

The photovoltage response signal decay for the dyad monolayers followed the power law, $U(t) \sim t^{-b}$, with the b values of approximately 0.25 [27]. In the PHT–dyad systems, the photovoltage decay is slower than that for the monolayer as seen in Fig. 4. For the PHT–ZnDHD6ee, the decay in double logarithmic scale does not follow exactly the power law as it is for the ZnDHD6ee monolayer, but is rather a two exponential with different exponents, first 0.05 and then changes at approximately 30 μs after excitation to a value of 0.13. The observed PV decays indicate that the charge migration and the charge recombination are more complex in the bi-layer system than in the dyad monolayer. For example, the charge migration can take place in more than two layers in the bi-layers.

3.2.2. Photocurrent response

For the pair of the complementary PHT–DHD6ee bi-layer samples, oppositely deposited onto ITO electrode, the photocurrent signals were measured in the light on/off mode and typical results are presented in Fig. 5. The obtained signals with opposite signs indicate that the deposition directions of the DA dyad layer determine the direction of the electron transfer in the triad system. At the moment the light is switched on the charge transfer reaction starts. Under the light illumination both the charge separation and the charge recombination processes are running in the bi-layer structure. Due to the insulating layers on both sides of the active layers there is no static current through the sample and the response current obtains a constant value when equilibrium, i.e. steady-state, between the formation and recombination processes of the CS state is reached. When the light is switched off the reached equilibrium is disturbed and the charge recombination results in a transient current signal with opposite sign than that characterizing the photogeneration of CS states.

The studied system can be described by a simple model of a three-state system (Scheme 3), the ground state (N), the excited state (N^*) and the CS state (N_{CS}). The total number of states in the system is $N_0 = N + N^* + N_{CS}$. The excited state is formed after excitation and relaxes to the CS state with a rate constant k_{CS} and directly to the ground state with a rate constant k_d. Thus, the differential rate law for the excited state population is $dN^*/dt = \alpha PN - (k_{CS} + k_d)N^*$, where $\alpha = \sigma/h\nu$, σ is the absorption cross-section, $h\nu$ the photon energy and P is the excitation power density. Since the system is excited with a continuous light the formation and the relaxation rates reach an equilibrium in time which can be expected to be much shorter than the time resolution of the PC measurement. In other words, $dN^*/dt = 0$ and concentration of the excited state is $N^* = N\alpha P/(k_d + k_{CS})$.

The measured current, J, is proportional to the rate of population change (dN_{CS}/dt) of the CS state. The CS population change is $dN_{CS}/dt = k_{CS}N^* - k_0N_{CS}$, where k_0 is the recombination rate constant for the CS state. When taken into account the value of N^*, the total number of the states can be given by $N_0 = N + N_{CS} + N\alpha P/(k_d + k_{CS})$. From these one will obtain an equation for the photocurrent decay

$$J = \frac{dQ}{dt} \propto \frac{dN_{CS}}{dt} = \left[\alpha P \frac{k_{CS} + k_0}{k_{CS} + k_d} + k_0\right] N - k_0 N_0. \quad (1)$$

Formation of the CS state in solutions is of the order of 10^{11} s^{-1} [20]. From the PV decays (Fig. 2) one can observe that the charge recombination is several orders of magnitude slower and $k_0 \ll k_{CS}$. Thus the ratio $(k_{CS} + k_0)/(k_{CS} + k_d) = k_{CS}/$

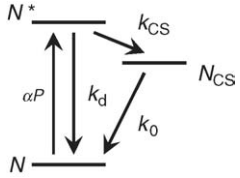

Scheme 3.

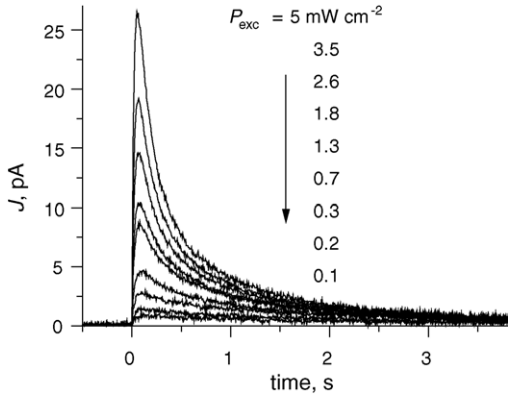

Fig. 6. Photocurrent response signals for the bi-layer sample DHD6ee (down)/PHT (up). The excitation light at 430 nm was switched on at $t = 0$. The responses were recorded with different excitation power densities (0.1–5 mW cm^{-2}).

$(k_{CS} + k_d) = \phi_{CS}$, the quantum yield of the CS state formation. Eq. (1) can be re-written as:

$$\frac{dN_{CS}}{dt} = [\phi_{CS}\alpha P + k_0]N - k_0 N_0. \quad (2)$$

The PC response signal decay rate, k, is proportional to the excitation light power density, P, as follows:

$$k = k_0 + \phi_{CS}\alpha P. \quad (3)$$

The photocurrent response signals for the sample with structure ITO|ODA|DHD6ee (down)|PHT (up)|ODA|Al measured at different excitation intensities are shown in Fig. 6. Similar measurements were done for the complementary PHT–DHD6ee bi-layer sample. In order to calculate the values for k, Eq. (3) the PC response signals were fitted with two exponential fit $J(t) = \sum a_i \exp[-tk_i] + C$ for each sample. The first exponential corresponds the rise of the signal, $k_1 = \tau_{RC}{}^{-1}$, and the second the decay of the PC signal. The constant C describes the remaining portion of the PC signal level corresponding the potential at the equilibrium. The obtained rate constants, k, were plotted as a function of excitation density (Fig. 7) and Eq. (3) was applied.

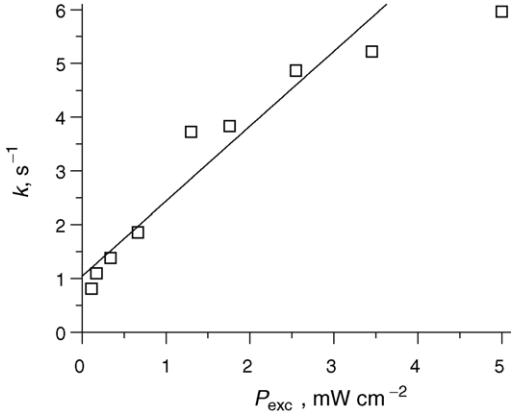

Fig. 7. Dependence of photocurrent decay rate, k, on the excitation intensity for the bi-layer DHD6ee (down)/PHT (up). The solid line shows the approximation for the rate constant.

Table 1
Approximations for the charge recombination rate constants, k_0, for different bi-layers

Bi-layer	k_0 (s^{-1})	$\phi_{CS}\alpha$ (s^{-1} mW^{-1} cm^2)	ϕ_{CS}
DHD6ee (down)/PHT (up)	0.83	1.40	0.84
PHT (down)/DHD6ee (up)	0.91	1.24	0.75

The values for coefficient $\phi_{CS}\alpha$ and for the computational CS quantum yield, ϕ_{CS}.

From the linear fits applying Eq. (3) the obtained charge recombination rates, k_0, have value roughly 0.9 s^{-1} for both bi-layer systems (Table 1). Such long-living CS states are obviously due to the interlayer charge transfer in the bi-layer system. The lateral movement of the generated positive charges in the conjugated π-system of the conductive polymer and the electrons in the fullerene network, increases further the lifetimes.

The linear fits with Eq. (3) give the slopes = $\phi_{CS}\alpha$ for different sample systems. They are listed in Table 1. In order to determine the quantum yield one needs an estimation for the cross-section, σ. The value for the cross-section, σ, obtained from the absorption measurements is 0.77×10^{-15} cm^2 for DHD6ee [27]. By using these values the quantum yields obtain values of approximately 0.8. The quantum yield values close to unity indicate efficient CS state formation.

3.2.3. PC action spectrum

The photocurrent responses for the complementary PHT–DHD6ee bi-layer samples were recorded at different excitation wavelengths in order to measure the PC action spectra. The obtained maximum current values as a function of the wavelength were corrected with the power spectrum of the excitation source. The spectra for the DHD6ee containing bi-layer samples are shown in Fig. 8. The action spectra have well-pronounced Soret band, but in the range of 500–600 nm the photocurrent spectra do not coincidence with the PHT absorption band showing smaller contribution of PHT on the PC signal. One can conclude that the vectorial photoinduced electron transfer in the bi-layer structure results from the primary electron transfer from excited porphyrin to fullerene

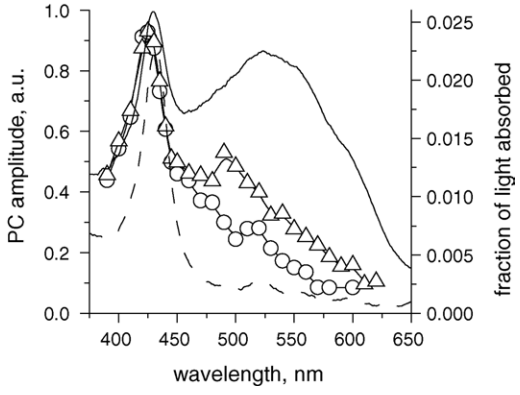

Fig. 8. Photocurrent action spectra for the bi-layers DHD6ee (down)/PHT (up) and PHT (down)/DHD6ee (up) are shown with circles and triangles, respectively. The absorption spectra for the DHD6ee monolayer and the PHT–DHD6ee bi-layer are shown with dotted and solid lines, respectively.

followed by the secondary electron transfer from PHT to the porphyrin cation. The low PC amplitude at the range 500–600 nm, compared to the PHT absorption, suggest that the direct electron transfer from PHT to fullerene is less probable.

4. Conclusions

The molecular bi-layer system consisting of porphyrin–fullerene dyad and PHT monolayers undergoes multistep vectorial photoinduced electron transfer with yield close to unity. After photoexcitation the primary electron transfer takes place in the porphyrin–fullerene molecule from the excited porphyrin to the fullerene. Next step is a secondary electron transfer from the PHT to the porphyrin cation. The resulting charge-separated state has lifetime close to second, which is due to the charge migration in the fullerene and polymer networks.

Acknowledgements

This work was supported by the Academy of Finland, Project "New Artificial Donor–Acceptor Materials" and the National Technology Agency of Finland.

References

[1] H. Imahori, M. Hagivara, M. Aoki, T. Akiyma, S. Tanigushi, T. Okada, M. Shirakava, Y.J. Sakata, J. Am. Chem. Soc. 118 (1996) 11771–11782.
[2] H. Yamada, H. Imahori, Y. Nishimura, I. Yamasaki, T.K. Ahn, S.K. Kim, D. Kim, S. Fukuzumi, J. Am. Chem. Soc. 125 (2003) 9129–9139.
[3] M.A. Loi, P. Denk, H. Hoppe, H. Neugebauer, C. Winder, D. Meissner, C. Brabec, N.S. Sariciftci, A. Gouloumis, P. Vázquez, T. Torres, J. Mater. Chem. 13 (2003) 700–704.
[4] D.M. Guldi, I. Zilbermann, A. Gouloumis, P. Vázquez, T. Torres, J. Phys. Chem. B 108 (2004) 18485–18494.
[5] T. Galili, A. Regev, H. Levanon, D.I. Schuster, D.M. Guldi, J. Phys. Chem. A 108 (2004) 10632–10639.
[6] Y. Araki, H. Luo, T. Nakamura, M. Fujitsuka, O. Ito, H. Kanato, Y. Aso, T. Otsubo, J. Phys. Chem. A 108 (2004) 10649–10655.
[7] J.L. Bahr, G. Kodis, L. de la Garza, S. Lin, A.L. Moore, T.A. Moore, D. Gust, J. Am. Chem. Soc. 123 (2001) 7124–7133.
[8] H. Imahori, H. Yamada, Y. Nishimura, I. Yamazaki, Y. Sakata, J. Phys. Chem. B 104 (2000) 2099–2108.
[9] F. D'Souza, G.R. Deviprasad, M.E. Zandler, M.E. El-Khouly, M. Fujitsuka, O. Ito, J. Phys. Chem. B 106 (2002) 4952–4962.
[10] J. Ikemoto, K. Takimiya, Y. Aso, T. Otsubo, M. Fujitsuka, O. Ito, Org. Lett. 4 (2002) 309–311.
[11] M. Isosomppi, N.V. Tkachenko, A. Efimov, H. Lemmetyinen, J. Phys. Chem. A 109 (2005) 4881–4890.
[12] T.D.M. Bell, K.A. Jolliffe, K.P. Ghiggino, A.M. Oliver, M.J. Shephard, S.J. Langford, M.N. Paddon-Row, J. Am. Chem. Soc. 122 (2000) 10661–10666.
[13] D.M. Guldi, H. Imahori, K. Tamaki, Y. Kashiwagi, H. Yamada, Y. Sakata, S. Fukuzumi, J. Phys. Chem. A 108 (2004) 541–548.
[14] V. Vehmanen, N.V. Tkachenko, H. Imahori, S. Fukuzumi, H. Lemmetyinen, Spectrochim. Acta A 57 (2001) 2229–2244.
[15] A. Efimov, P. Vainiotalo, N.V. Tkachenko, H. Lemmetyinen, H.J. Porphyrins, Phthalocyanines 7 (2003) 610–616.
[16] D. Kuciauskas, S. Lin, G.R. Seely, A.L. Moore, T.A. Moore, D. Gust, T. Drovetskaya, C.A. Reed, P.D.W. Boyd, J. Phys. Chem. 100 (1996) 15926–15932.
[17] E. Dietel, A. Hirsch, J. Zhou, A. Rieker, J. Chem. Soc., Perkin Trans. 2 6 (1998) 1357–1364.
[18] K. Yamada, H. Imahori, Y. Nishimura, Y. Sakata, Chem. Lett. 28 (1999) 895–896.
[19] S. Fukuzumi, H. Imahori, H. Yamada, M.E. El-Khouly, M. Fujitsuka, O. Ito, D.M. Guldi, J. Am. Chem. Soc. 123 (2001) 2571–2575.
[20] V. Chukharev, N.V. Tkachenko, A. Efimov, D.M. Guldi, A. Hirsch, M. Scheloske, H. Lemmetyinen, J. Phys. Chem. B 108 (2004) 16377–16385.
[21] G. Roberts, Langmuir–Blodgett Films, Plenum Press, New York, 1990.
[22] N.V. Tkachenko, E. Vuorimaa, T. Kesti, A.S. Alekseev, A.Y. Tauber, P.H. Hynninen, H. Lemmetyinen, J. Phys. Chem. B 104 (2000) 6371–6379.
[23] A.S. Alekseev, N.V. Tkachenko, A.Y. Tauber, P.H. Hynninen, R. Osterbacka, H. Stubb, H. Lemmetyinen, Chem. Phys. 275 (2002) 243–251.
[24] N.V. Tkachenko, V. Vehmanen, A. Efimov, A.S. Alekseev, H. Lemmetyinen, J. Porphyrins Phthalocyanines 7 (2003) 255–263.
[25] T. Ito, I. Yamazaki, N. Ohta, Chem. Phys. Lett. 277 (1997) 125–131.
[26] T. Ito, I. Yamazaki, N. Ohta, J. Phys. Chem. B 106 (2002) 895–898.
[27] T. Vuorinen, K. Kaunisto, N.V. Tkachenko, A. Efimov, A.S. Alekseev, K. Hosomizu, H. Imahori, H. Lemmetyinen, Langmuir 21 (2005) 5383–5390.
[28] M. Ahlskog, J. Paloheimo, H. Stubb, P. Dyreklev, M. Fahlman, O. Ingranars, M.R. Andersson, J. Appl. Phys. 76 (1994) 893–899.
[29] N.V. Tkachenko, P.H. Hynninen, H. Lemmetyinen, Chem. Phys. Lett. 261 (1996) 234–240.
[30] I. Watanabe, K. Hong, M.F. Rubner, Langmuir 6 (1990) 1164–1172.